Thermal measurements of a one-dimensional wire in the quantum limit



2008 J. Phys.: Condens. Matter 20 164210

(http://iopscience.iop.org/0953-8984/20/16/164210)

IOP PUBLISHING JOURNAL OF PHYSICS: CONDENSED MATTER

J. Phys.: Condens. Matter **20** (2008) 164210 (7pp) doi:10.1088/0953-8984/20/16/164210

# Thermal measurements of a one-dimensional wire in the quantum limit

**J T Nicholls and O Chiatti**[1]

Department of Physics, Royal Holloway, University of London, Egham, Surrey TW20 0EX, UK

E-mail: james.nicholls@rhul.ac.uk

Received 17 October 2007, in final form 7 December 2007
Published 1 April 2008
Online at stacks.iop.org/JPhysCM/20/164210

**Abstract**

The single-particle properties of a ballistic one-dimensional (1D) conductor are reviewed; the breakdown in these properties is used to characterize the *0.7 structure*, an anomalous but reproducible feature in the conductance $G$ that is measured at $G = 0.7 \times 2e^2/h$.

We show how alternating current heating creates a temperature difference $\Delta T$ across a 1D wire, allowing thermopower measurements. The thermopower characteristics $S(V_g)$ show deviations from Cutler–Mott predictions (a single-particle theory) close to the 0.7 structure. The magnitude of a thermovoltage peak is used to measure the electron temperature, and we have incorporated a mesoscopic thermometer into a simple thermal circuit that allows us to measure the thermal conductance of a 1D wire. For the first four 1D subbands the heat carried by electrons passing through the 1D constriction is proportional to the electrical conductance $G(V_g)$; this is the first demonstration that the thermal conductance due to electrons is quantized. In the vicinity of the 0.7 structure the Wiedemann–Franz ratio breaks down, and a plateau at the quantum of thermal conductance $\pi^2 k_B^2 T/3h$ is observed.

## 1. Introduction

Ballistic one-dimensional (1D) conduction quantized in units of $G_0 = 2e^2/h$ was discovered [1, 2] using split-gates deposited on the sample surface of a GaAs-based two-dimensional electron gas (2DEG). Since that time many devices have been fabricated with different parameters: length $L$ and width $W$ of the split-gate, depth $d$ and quality (typically mobility $\mu$) of the 2DEG, etc. Conductance measurements $G(V_g)$ are the simplest and most revealing experiment to perform on any newly fabricated sample, where the presence or absence of conductance plateaus in $G(V_g)$ can quickly determine the quality of the sample. If the 1D constriction is free from impurities and there is little subband mixing, clean conductance plateaus will be measured, and in exceptional cases more than thirty plateaus have been observed [3].

The 0.7 structure is a reproducible feature observed near $0.7G_0$ in the conductance characteristics $G(V_g)$ of clean 1D samples. There is evidence that it has a spin origin and recent shot-noise measurements [4] show that the 0.7 structure could be interpreted assuming two conducting channels (spin-up $\uparrow$ and spin-down $\downarrow$) that have different transmission probabilities. The 0.7 structure could be evidence [5, 6] for a spontaneous static spin polarization within the lowest 1D subband, but the plateau-like structure occurs at $0.7G_0$ rather than at $e^2/h$, and moreover the temperature dependence suggests that the 0.7 structure is not a ground-state property. Since its discovery the 0.7 structure has been observed in clean GaAs wires made by different fabrication routes—there is however no single mechanism (static [5], dynamic [7], or otherwise) that can account for all the experimental observations.

By way of introduction we review some of the single-particle properties of a 1D ballistic constriction.

(i) In clean short 1D wires there are conductance steps at integer multiples of $2e^2/h$, observed as the gate voltage $V_g$ is swept more negative [1, 2]. As $V_g$ is swept towards pinch-off ($G = 0$) both the width of the 1D channel and the local electron density in the constriction are reduced. In the Landauer picture each $2e^2/h$ drop in the conductance corresponds to the depopulation of a spin-degenerate 1D subband.

[1] Present address: Hochfeld-Magnetlabor Dresden, Forschungszentrum Dresden-Rossendorf (FZD), D-01314 Dresden, Germany.

 

(ii) With increasing temperature, the Fermi functions which describe the electron energy distribution in the source and drain become broadened—this in turn smears the distinction between the plateaus and risers in the conductance characteristics $G(V_g)$. At high temperatures when $k_B T \gg E_N - E_{N-1}$, where $E_N$ is the energy of the $N$th 1D subband, the plateaus disappear and the $G(V_g)$ traces become featureless.

(iii) The application of a strong magnetic field $B_\parallel$, applied parallel to the plane of the 2DEG, lifts the spin degeneracy of the 1D subbands. The Zeeman energy $2g\mu_B B_\parallel S$ and hence the $g$-factors, can be measured using a source–drain voltage $V_{sd}$. For the higher subbands ($N \gg 1$) it is found [5] that $g \approx 0.4$, close to the bulk GaAs value.

(iv) The application of a DC source–drain voltage $V_{sd}$, on top of the usual AC measuring voltage, opens up a window of energy $eV_{sd}$ about the Fermi energy. Non-equilibrium studies ($V_{sd} \neq 0$) for conductances $G > 2e^2/h$ show that half-plateaus result from the differing occupations of the 1D subbands in the two transport directions, all of which can be understood within the single-particle picture [8]. The DC source–drain voltage $V_{sd}$ can be used to follow the energy subbands as a function of gate voltage $V_g$. The transconductance $dG/dV_g$ can be plotted as a function of both $V_g$ and $V_{sd}$, yielding diamond-shaped grey scale plots; these show that the 1D subbands move linearly with gate voltage.

The counterparts to the above properties are listed below for the 0.7 structure:

(i) There is a reproducible structure in the conductance around $0.7 \times 2e^2/h$—the quantization is not as accurate as that of the single-particle steps at multiples of $2e^2h$. What is clear is that the 0.7 structure occurs between $e^2/h$ and $2e^2/h$, which in the Landauer picture means that there are between one and two conducting spin-split 1D subbands contributing to the conductance.

(ii) Unusually the 0.7 structure becomes stronger with temperature [5], a result most clearly demonstrated [9] in etched samples which have strong lateral confinement.

(iii) With the application of a strong parallel magnetic field, $B_\parallel$, the 0.7 structure shifts down in conductance, eventually evolving into the spin-split plateau at $e^2/h$. Using equilibrium measurements ($V_{sd} = 0$) the gate voltage splitting of the $dG/dV_g$ peaks give an indication of the energy splitting. By following this energy splitting with increasing magnetic field, see figure 1, the 0.7 structure at low fields evolves into the usual spin-split subbands at high fields. In addition the in-plane $g$-factors measured in the last subbands are found to be enhanced [5] over the values measured when $N \gg 1$.

(iv) Upon application of a source–drain voltage $V_{sd}$ the features in the grey scale plots associated with the spin-up and spin-down 1D subbands show non-linearities and abrupt changes as they are populated or depopulated [10].

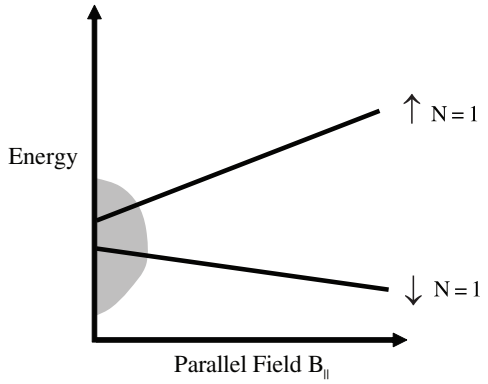


**Figure 1.** Schematic of the energy splitting between the spin-up (↑) and spin-down (↓) energy levels within the last ($N = 1$) conducting subband, as a function of the applied parallel magnetic field $B_\parallel$. In a strong $B_\parallel$ field the ↑ and ↓ subbands are separated by the Zeeman energy $E_Z$ and the $G(V_g)$ trace exhibits plateaus at $e^2/h$ and $2e^2/h$. As the magnetic field is reduced the Zeeman splitting decreases linearly; however in the limit of zero magnetic field there is a finite offset. This result suggests that the Zeeman energy has the form $E_Z = 2g\mu_B B_\parallel S + C$, where the constant $C$ could be interpreted [5] as evidence for zero-field spin-splitting; unfortunately for this interpretation the conductance exhibits a plateau at $0.7 \times (2e^2/h) = 1.4(e^2/h)$ rather than at $e^2/h$. The shaded area shows schematically the region where the single-particle properties breakdown, extending out to a couple of Tesla in $B_\parallel$.

## 2. Current heating and thermopower measurements

Not long after the discovery of ballistic conduction, Molenkamp and co-workers [11] performed thermopower measurements, $S(V_g)$, as well as preliminary thermal conductance $\kappa(V_g)$ measurements. The early measurements were performed at gate voltages well away from the last conducting subband, and were in agreement with theory. The theory for describing these transport coefficients was put on a firm footing [12] within the Landauer–Büttiker theory.

In this paper we review our recent thermal measurements, highlighting the deviations from single-particle behaviour which occur at and around the 0.7 structure. Thermal measurements are in general more difficult to carry out than electrical measurements, even more so when performed close to pinch-off ($G \to 0$). For example, both spurious and nonlinear thermovoltages can be created by the rising capacitance of the split-gate, and the poor definition of the electrical earth on the heated side of the sample (necessary to sink $I_H$).

Thermal measurements require an electron temperature difference $\Delta T$, from one side of the 1D wire to the other, between the source and drain. Fortunately this can be readily achieved by passing a current $I_H$ between the Ohmic contacts on one side of the sample; the resulting Joule heating ($I_H^2 R$) raises the electron temperature on that side, and because of the weak coupling between the electrons and the lattice, the lattice temperature $T_L$ remains unchanged throughout the sample. The electron temperature on the unheated side of the 1D channel remains at the lattice (bath) temperature $T_L$, whereas the electrons on the heated side have a temperature $T_e$; the temperature difference across the sample is $\Delta T = T_e - T_L$. The

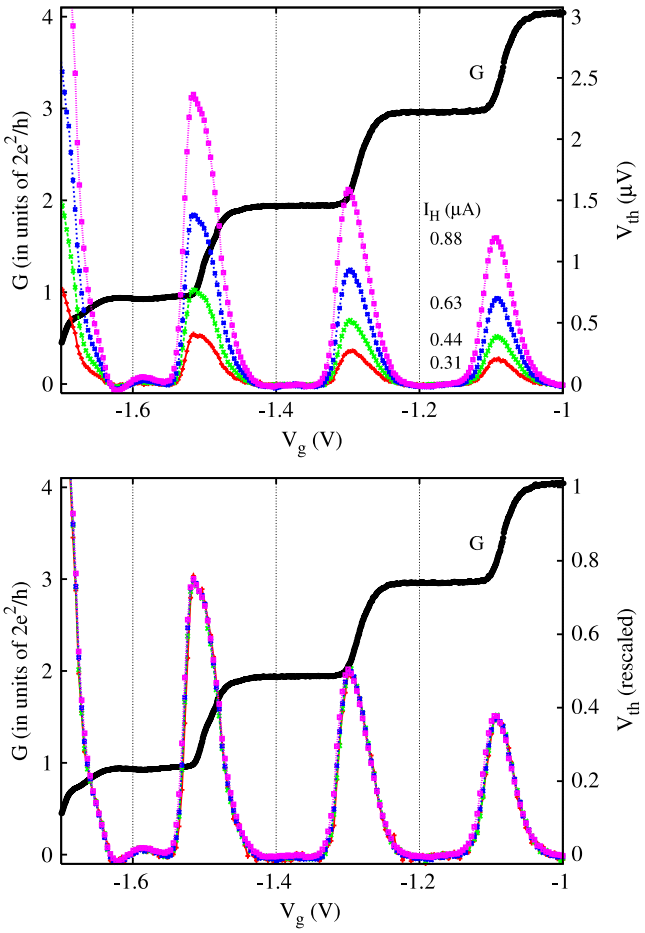


**Figure 2.** Upper: raw thermovoltage traces $V_{\rm th}(V_{\rm g})$ of a ballistic 1D wire at $T = 0.3$ K, obtained using heating currents of $I_{\rm H} = 0.31$, 0.44, 0.63 and 0.88 $\mu$A. Lower: the scaled thermovoltage, obtained by dividing each raw $V_{\rm th}$ trace by its value at $V_{\rm g} = -1.7$ V. The scaled data all collapses onto a single curve, demonstrating that the $V_{\rm th}$ measurements are linear.

(This figure is in colour only in the electronic version)

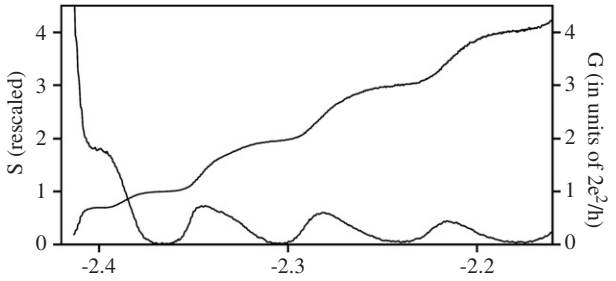


**Figure 3.** Simultaneous thermopower $S$ and conductance $G$ measurements at $T = 0.3$ K of a 1D constriction close to pinch-off [14]. According to the Cutler–Mott relation (equation (1)) a plateau in $G$ should be accompanied by a zero in $S$—this prediction holds for the plateaus at $N \times 2e^2/h$ for $N = 1$, 2, 3, and 4, but breaks down on the 0.7 structure at $V_{\rm g} = -2.4$ V.

electron–electron scattering rate is much faster than all other scattering rates, so all of the electrons on the heated side of the sample will equilibrate at a local temperature $T_{\rm H} = T_{\rm L} + \Delta T$. Either AC or DC heating currents $I_{\rm H}$ can be used, though better signal-to-noise measurements can be achieved using lock-in techniques to measure a thermovoltage $V_{\rm th}$ at frequency $2f$, in response to electron heating by a current $I_{\rm H}$ at frequency $f$.

The simplest measurement that can be performed using current heating is that of the thermopower, $S = -(V_{\rm th}/\Delta T)_{I=0}$, where the applied temperature difference $\Delta T$ induces a thermovoltage $V_{\rm th}$ across the 1D wire. In linear response $S$ is related to the conductance $G = (\delta I/\delta V)_{\delta T=0}$ through the relation [13]

$$S = -\frac{\pi^2 k_{\rm B}^2 T}{3e}\frac{1}{G}\frac{\partial G}{\partial \mu}, \qquad (1)$$

where $\mu$ is the chemical potential.

Figure 2 shows typical traces of the raw thermovoltage $V_{\rm th}$ and conductance $G$ for a 1D constriction, where the traces are obtained at different heating currents $I_{\rm H}$. There is a peak in $S(V_{\rm g})$ (and also in $V_{\rm th}(V_{\rm g})$) where there is a riser (or step) in the conductance $G(V_{\rm g})$, all in agreement with equation (1). The upper part of figure 2 shows the raw thermovoltage traces $V_{\rm th}(V_{\rm g})$ at $T = 0.3$ K, obtained using the heating currents $I_{\rm H} = 0.31, 0.44, 0.63$ and 0.88 $\mu$A. Clearly as the heating current increases, the electrons on one side of the sample are heated to a temperature $\Delta T$ above the lattice temperature $T_{\rm L}$, and the resulting thermopower peaks become stronger. The lower part of figure 2 shows the scaled thermovoltage, obtained by dividing each $V_{\rm th}$ trace by its value at $V_{\rm g} = -1.7$ V; the scaled data all collapses onto a single curve, demonstrating that the $V_{\rm th}$ measurements are linear. The height of a thermovoltage peak can be used as an electron thermometer, as will be demonstrated in the thermal conductance measurements in section 3. The electron thermometer generates a thermovoltage which is of the order of a few $\mu$V or less, for a $\Delta T$ of 100 mK.

Equation (1) was derived for a non-interacting, degenerate electron gas and has been reformulated [15–17] for a mesoscopic device connected to Fermi function reservoirs; it is found that it remains essentially unchanged. We note that a careful analytical and numerical study [18] shows that for non-interacting electrons it is alright to use a finite temperature (rather than a zero temperature) conductance in equation (1). One possible approach would be to use this equation to identify where single-particle theory breaks down. Figure 3 shows simultaneous thermopower $S$ and conductance $G$ traces of a different 1D wire close to pinch-off at $T = 0.3$ K, which shows a particularly well developed 0.7 structure that is almost a plateau. According to the Cutler–Mott relation (equation (1)) a plateau in the conductance should be accompanied by a zero in the thermopower—such a prediction holds for the plateaus at $N \times 2e^2/h$ for $N = 1, 2, 3$, and 4, but breaks down for the 0.7 structure at $V_{\rm g} = -2.4$ V. Reference [14] shows that in a strong $B_\parallel$ field the 0.7 structure in $G$ shifts down to $e^2/h$ and the thermopower $S$ develops a zero, consistent with a return to single-particle behaviour at high fields (as shown in figure 1). It is not theoretically known why there is an enhanced thermopower on the 0.7 structure. One could speculate that additional degrees of freedom, for example, magnetic excitations could make a contribution to $S$, but as yet no firm theories have been put forward.

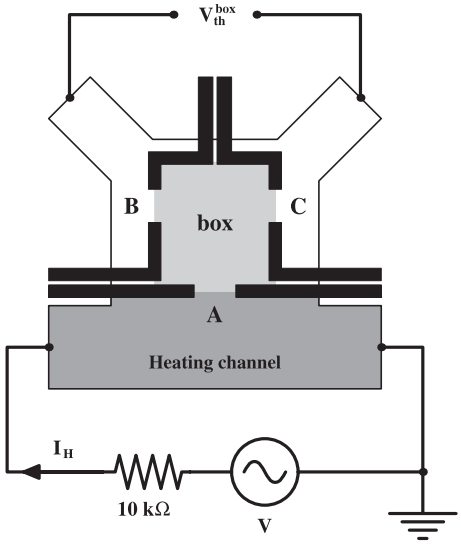


**Figure 4.** Schematic of the device and set-up for thermal conductance $\kappa(V_g)$ measurements. Electrons can only pass through the constrictions labelled A, B and C; the much narrower channels are pinched-off. Electrons in the heating channel are heated to $T_H = T_L + \Delta T$ by a current $I_H$; hot electrons pass through the sample constriction (A) into the box, where the temperature $T_{box} = T_L + \delta T$ is determined by the thermovoltage $V_{th}^{box}$ generated across constrictions B and C.

## 3. Thermal conductance measurements

In this section we introduce a device in which we can directly compare thermal $\kappa(V_g)$ and electrical $G(V_g)$ conductance measurements. Such a comparison is important because if both charge and energy are transported by electrons, there is a universal relation between $\kappa$ and $G$ known as the Wiedemann–Franz (WF) relation

$$\frac{\kappa}{GT} = \frac{\pi^2 k_B^2}{3e^2} = L_0, \tag{2}$$

where $L_0$ is the Lorenz number and $T$ is the temperature. Deviations from the WF ratio have been used to investigate non-Fermi liquid behaviour in a variety of condensed matter systems. Equation (2) predicts that the observation of conductance plateaus (in units of $G_0$) should be matched by steps in the thermal conductance, quantized in units of $L_0 T \times G_0 = (1.89 \times 10^{-12}\ \mathrm{W\,K^{-2}})T$.

To measure the thermal conductance we modify previous devices [11] by introducing a closed electron box whose temperature $T_{box}$ is measured by the electron thermometer [19, 20] described in section 2. Figure 4 shows a schematic of the 6 $\mu$m × 10 $\mu$m box, around which there are three split-gates, each with a gap that is 0.5 $\mu$m long and 0.65 $\mu$m wide. An AC current $I_H$ heats electrons in the heating channel to a temperature $T_H = T_L + \Delta T$. The electrons in the closed box have a well defined temperature, and for a given $I_H$ the thermovoltage generated is much larger than in more open structures [11].

Hot electrons in the heating channel can enter the box through constriction A (called the *sample* constriction) and can leave the box via constrictions B and C. In steady-state the heat flow in and out of the box is equal such that

$$\kappa_A(T_H - T_{box}) = (\kappa_B + \kappa_C)(T_{box} - T_L), \tag{3}$$

where $\kappa_A$, $\kappa_B$ and $\kappa_C$ are the thermal conductances of the three constrictions. The increase in the box temperature $T_{box} = T_L + \delta T$ is given by

$$\delta T = \frac{\kappa_A}{\kappa_A + \kappa_B + \kappa_C} \times \Delta T. \tag{4}$$

Constrictions B and C (defined as the *thermometer* and *reference* constrictions) are used to measure $T_{box}$. The temperature rise $\delta T$ within the box generates a thermovoltage in both B and C, but constriction C is put on a conductance plateau so its contribution (see equation (1)) is zero [20]. Therefore the measured thermovoltage is solely due to constriction B

$$V_{th}^{box} = S_B(T_{box} - T_L) = S_B\,\delta T. \tag{5}$$

The thermopower $S_B$ is proportional to the average of the temperatures on either side of constriction B, allowing equation (5) to be rewritten as

$$V_{th}^{box} = c_B(T_{box}^2 - T_L^2), \tag{6}$$

where the calibration constant, $c_B \approx 15\ \mu\mathrm{V\,K^{-2}}$, is determined by DC source–drain voltage measurements of the subband spacing [20]. When constriction A is not defined, the electron thermometer is in direct contact with the heating channel, and the thermovoltage $V_{th}^{H}$ at this gate voltage is a measure of $T_H$ through the relation

$$V_{th}^{H} = c_B(T_H^2 - T_L^2). \tag{7}$$

Equations (4) and (5) show that measurements of $V_{th}^{box}(V_g)$, and hence $\delta T$, lead directly to the thermal conductance $\kappa_A(V_g)$, provided we know $\Delta T$ and make certain assumptions about $\kappa_B$ and $\kappa_C$.

Figure 5 shows the raw thermovoltage $V_{th}^{box}(V_g)$ traces taken as the gate voltage $V_g$ of constriction A is swept, while constrictions B and C are set at $G_B = 1.5G_0$ and $G_C = G_0$, respectively. The steps in $V_{th}^{box}$ are aligned with those in the conductance $G_A$ (top trace), confirming that the structure in $V_{th}^{box}$ is due to the 1D subbands. Traces (a)–(d) were obtained with heating currents $I_H = 0.2$–$1\ \mu$A, and the corresponding temperature rise in the heating channel $\Delta T = 15$–$100$ mK were calculated using equation (6).

The thermovoltage $V_{th}^{box}$ shown in figure 5 follows the shape of the conductance characteristics $G_A(V_g)$; as well as the steps, the definition of constriction A at $V_g \approx 0.3$ V can be seen in all the traces. At $V_g = 0.5$ V both constriction A and the box are not defined, and the electron thermometer is in direct contact with the heating channel; we define $V_{th}^{box}(V_g = 0.5\ \mathrm{V}) = V_{th}^{H}$, and $T_H$ is obtained using equation (7). There are also energy losses from hot electrons to the lattice via the electron–phonon interaction ($\propto T^5$)—we have previously measured [20] these and they can be neglected for $T < 0.5$ K.

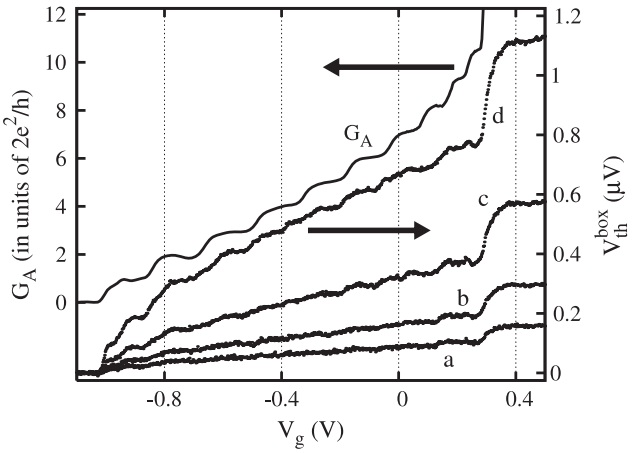


**Figure 5.** The thermovoltage $V_{\rm th}^{\rm box}$ of the electron box together with the conductance $G_{\rm A}$, measured at a lattice temperature $T_{\rm L} = 0.27$ K using heating currents of (a) $I_{\rm H} = 0.2$ $\mu$A, (b) 0.3 $\mu$A, (c) 0.5 $\mu$A, and (d) 1 $\mu$A. The corresponding temperature rises were estimated to be $\Delta T = 15$, 30, 55, and 100 mK, respectively. The thermovoltage approximately scales with $I_{\rm H}^2$ up to $I_{\rm H} = 1$ $\mu$A [21].

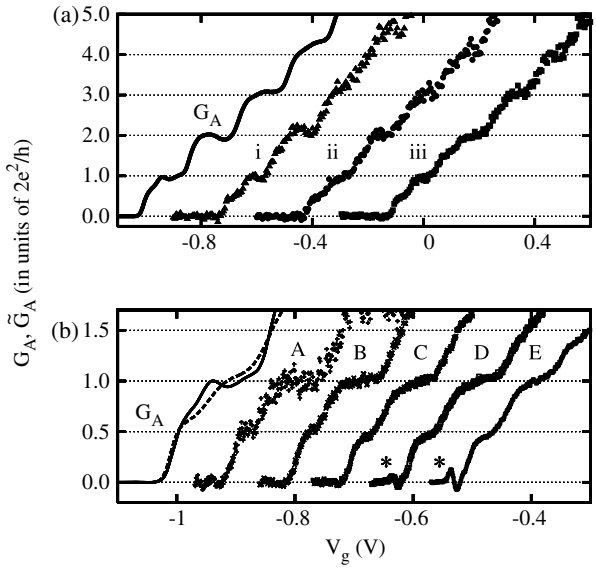


**Figure 6.** (a) The thermally derived conductance $\tilde{G}_{\rm A}(V_{\rm g})$ and electrical conductance $G_{\rm A}(V_{\rm g})$ of constriction A at $T_{\rm L} = 0.27$ K [21]. Left solid line: conductance $G_{\rm A}(V_{\rm g})$. Measurements of $\tilde{G}_{\rm A}(V_{\rm g})$ were obtained with $I_{\rm H} = 1$ $\mu$A, $G_{\rm B} = 1.5G_0$ and $G_{\rm C} = 3G_0$ (trace i), $G_{\rm C} = 4G_0$ (trace ii) and $G_{\rm C} = 5G_0$ (trace iii). For clarity successive traces have been shifted by 0.3 V to the right. (b) The thermal and electrical conductances close to pinch-off, showing that at the gate voltage corresponding to the 0.7 structure, $\tilde{G}_{\rm A}$ exhibits a half-plateau. Far left traces: $G_{\rm A}(V_{\rm g})$ at $T_{\rm L} = 0.3$ K (solid) and $T_{\rm L} = 1.2$ K (dashed). Traces A–E: $\tilde{G}_{\rm A}(V_{\rm g})$ at $T_{\rm L} = 0.27$ K for heating currents $I_{\rm H} = 0.2$, 0.4, 1, 2, and 3 $\mu$A; the corresponding $\Delta T$ are calculated to be 26, 66, 133, 193, and 234 mK. The $\tilde{G}_{\rm A}(V_{\rm g})$ traces A and B were obtained with $G_{\rm B} = 1.5G_0$ and $G_{\rm C} = 3G_0$; traces C–E were obtained with $G_{\rm B} = 1.5G_0$ and $G_{\rm C} = 2G_0$.

It is not possible to measure $\kappa_{\rm A}$, $\kappa_{\rm B}$ and $\kappa_{\rm C}$ independently, and so we assume that the thermal conductance of each constriction is proportional to its electrical conductance,

$$\kappa_j = \alpha_j G_j \overline{T}, \qquad j = \text{A, B or C} \tag{8}$$

where $\alpha_j$ is a constant and $\overline{T}$ is the average of the temperatures on either side of the $j$th constriction. Assuming that the WF ratio is the same for all three constrictions, $\alpha_{\rm A} = \alpha_{\rm B} = \alpha_{\rm C} = \alpha$, equation (3) can be written as

$$\tilde{G}_{\rm A} = (G_{\rm B} + G_{\rm C})\frac{T_{\rm box}^2 - T_L^2}{T_H^2 - T_{\rm box}^2} = (G_{\rm B} + G_{\rm C})\frac{V_{\rm th}^{\rm box}}{V_{\rm th}^{\rm H} - V_{\rm th}^{\rm box}}, \tag{9}$$

where $V_{\rm th}^{\rm box}(V_{\rm g})$ is measured as a function of the gate voltage on A, and $V_{\rm th}^{\rm H}$ is the thermovoltage when constriction A is not defined. If $G_{\rm B}$ and $G_{\rm C}$ are fixed at known conductances (usually constriction B is on a riser and C is on a plateau) the quantities $V_{\rm th}^{\rm H}$ and $V_{\rm th}^{\rm box}$ on the right side of equation (9) can be measured. The left side of equation (9) is written as $\tilde{G}_{\rm A}$, which is the expected conductance of constriction A as derived from thermal measurements. $\tilde{G}_{\rm A}(V_{\rm g})$ has the dimensions of conductance, and will be compared to the electrical conductance $G_{\rm A}(V_{\rm g})$.

Figure 6(a) shows traces of $\tilde{G}_{\rm A}$ (offset horizontally) compared to the electrical conductance $G_{\rm A}$, where the thermal data is taken with constriction B acting as the electron thermometer ($G_{\rm B} = 1.5G_0$) and the reference constriction C is set at $G_{\rm C} = 3G_0$ (trace i), $4G_0$ (trace ii) and $5G_0$ (trace iii). The increase in the box temperature, $\delta T$, as determined by equation (4) is different for each of the three traces, yet the same thermal conductance behaviour for constriction A is obtained, showing the validity of the technique. In comparison to the electrical conductance $G_{\rm A}$, which shows conductance plateaus at multiples of $G_0 = 2e^2/h$, there are three plateaus in $\tilde{G}_{\rm A}$ which occur (to within 10–15%) at similar multiples of $G_0$. The conductance characteristics $G_{\rm A}(V_{\rm g})$ in figure 6(a) show a 0.7 structure; there is, however, no corresponding 0.7 structure in the $\tilde{G}_{\rm A}(V_{\rm g})$ traces.

Figure 6(b) shows the conductances closer to pinch-off, where for clarity the $\tilde{G}_{\rm A}$ traces have been shifted to the right. The thermal conductances were measured at the lattice temperature $T_{\rm L} = 0.27$ K for different heating currents. At the lowest $I_{\rm H}$ (trace A) there is a discernible half-plateau at $e^2/h$ in $\tilde{G}_{\rm A}$, which corresponds in gate voltage to the 0.7 structure in $G_{\rm A}$. With increasing $I_{\rm H}$, traces B–E show less noise in $\tilde{G}_{\rm A}$, and the half-plateau in the thermal conductance is better resolved. This unexpected half-plateau in the thermal conductance was measured both in the linear regime, $(T_{\rm H} - T_{\rm box})/T_{\rm L} \sim 0.1$, but also persists into the non-linear regime where $(T_{\rm H} - T_{\rm box})/T_{\rm L} \sim 0.7$. To get some idea about the sensitivity of our thermal measurements, the heat flow $\dot{Q}$ through constriction A when the half-plateau in the thermal conductance is just distinguishable is $\dot{Q} = \kappa(T_{\rm H} - T_{\rm box}) \approx 6$ fW, more than two orders of magnitude smaller than previous measurements [11].

### *3.1. Discussion*

In the single-particle picture a breakdown of the WF relation is possible [22] if the transmission probability $t(E)$ of the constriction varies rapidly compared to the thermal energy difference across the constriction; however calculations for

the realistic saddle-point potential model of the constriction show [12] that there is no breakdown. First we discuss our thermal results for high conductances, $G > G_0$, where single-particle theory prevails. Figure 6(a) shows the measured behaviour with no adjustable parameters—there is an alignment of the first three conductance plateaus ($G_A = G_0, 2G_0$, and $3G_0$) with those in $\tilde{G}_A$, where the latter quantity is calculated from equation (9) assuming that all three constrictions behave similarly. The observed alignment cannot be interpreted as an absolute confirmation of the WF relation, because it is not known whether the constant of proportionality $\alpha$ (see equation (8)) is equal to the Lorenz number $L_0$. There is, however, no theoretical reason why the WF relation should not be obeyed for plateaus $G > G_0$.

It has been theoretically shown that in 1D the quantization of the thermal conductance is universal for thermal carriers that obey boson [23], fermion or anyon statistics [24]. Measurements have demonstrated this universality for phonons [25] and photons; [26] our thermal conductance measurements demonstrate this universality for electrons.

In long clean 1D wires Luttinger liquid behaviour is expected, and the resulting spin–charge separation causes the electrical and thermal conductances to behave differently, giving a breakdown of the WF relation and clearly demonstrating non-Fermi liquid behaviour [27]. In shorter 1D constrictions there is no accepted microscopic mechanism for the 0.7 structure, and we have found only one prediction for the thermal conductance. Assuming there is a weakly bound electron in the constriction Rejec *et al* [28] calculate that the normalized thermal conductance $\kappa/(L_0T)$ shows structure at $G_0/4$ and $3G_0/4$, and deviations from the WF law are expected at elevated temperatures. Our results do not show these fractional structures, but instead shows a feature at $\kappa/(L_0T) = G_0/2$. In the Landauer–Büttiker formalism the thermal conductance is calculated [12] to be

$$\kappa = TG_0(k_B/e)^2 \int_0^\infty t(E)\partial f/\partial E \epsilon^2 \mathrm{d}E, \qquad (10)$$

where $\epsilon = (E - E_F)/k_BT$, $f(\epsilon) = [\exp(\epsilon)+1]^{-1}$ is the Fermi function, and $E_F$ is the Fermi energy. In a phenomenological model [6] assuming a density dependent spin-gap, calculations of the electrical conductance $G = -G_0 \int_0^\infty t(E)\partial f/\partial E \, \mathrm{d}E$ show some similarity to $G(V_g)$ measurements of the 0.7 structure. We find that calculations using such a model gives a structure at $\kappa = L_0T \times 0.7G_0$; that is, the Wiedemann–Franz relation is obeyed and it is not possible to obtain simultaneous plateaus at $G = 0.7G_0$ and $\kappa = L_0T \times (G_0/2)$.

A plateau at $e^2/h = G_0/2$ has been measured in the electrical conductance of low density wires [29], longer wires [6], and symmetric wires [30], but in all cases it is not known whether there is a full spin polarization or some other state. A mechanism for an $e^2/h$ plateau in $G(V_g)$ has been put forward by Matveev [31, 32], where the 1D wire is modelled as a Wigner crystal in which there are separate charge and spin degrees of freedom. The electrical resistance has contributions from both, with the spin contribution being temperature dependent and going to zero when $T \to 0$.

## 4. Summary

We have described briefly how thermal measurements can be performed on 1D devices. Though these measurements are technically difficult, they do reveal deviations from single-particle behaviour at the 0.7 structure that support and extend the more straight forward electrical conductance characteristics. There is now a large collection of measurements on the 0.7 structure—there is a need that all this experimental evidence be considered in future theoretical models.

In particular we have presented measurements of the thermal conductance characteristics $\kappa(V_g)$. Over most of the gate voltage of a 1D wire the thermal conductance $\kappa$ follows the electrical conductance $G$ in accordance with equation (2). However, in the vicinity of the *0.7 structure* there is a breakdown of the Wiedemann–Franz relation, giving an unexpected plateau in thermal conductance at $L_0T \times (G_0/2)$. The techniques described here for measuring the thermal conductance could also be applied to quantum dots and long wires. It would also be interesting to perform $\kappa(V_g)$ measurements in a strong parallel magnetic field $B_\parallel$.

## Acknowledgments

This work was supported by the Engineering and Physical Sciences Research Council (UK). We acknowledge the contribution of collaborators at the Cavendish Laboratory (University of Cambridge) and Royal Holloway (University of London).

## References

[1] Wharam D A, Thornton T J, Newbury R, Pepper M, Ahmed H, Frost J E F, Hasko D G, Peacock D C, Ritchie D A and Jones G A C 1988 *J. Phys. C: Solid State Phys.* **21** L209

[2] van Wees B J, van Houten H, Beenakker C W J, Williamson J G, Kouwenhoven L P, van der Marel D and Foxon C T 1988 *Phys. Rev. Lett.* **60** 848

[3] Thomas K J, Simmons M Y, Nicholls J T, Mace D R, Pepper M and Ritchie D A 1995 *Appl. Phys. Lett.* **67** 109–11

[4] Roche P, Ségala J, Glattli D C, Nicholls J T, Pepper M, Graham A C, Thomas K J, Simmons M Y and Ritchie D A 2004 *Phys. Rev. Lett.* **93** 116602

[5] Thomas K J, Nicholls J T, Simmons M Y, Pepper M, Mace D R and Ritchie D A 1996 *Phys. Rev. Lett.* **77** 135–8

[6] Reilly D J, Facer G R, Dzurak A S, Kane B E, Clark R G, Stiles P J, Clark R G, Hamilton A R, O'Brien J L, Lumpkin N E, Pfeiffer L N and West K W 2001 *Phys. Rev.* B **63** 121311(R)

[7] Cronenwett S M, Lynch H J, Goldhaber-Gordon D, Kouwenhoven L P, Marcus C M, Hirose K, Wingreen N S and Umansky V 2002 *Phys. Rev. Lett.* **88** 226805

[8] Patel N K, Nicholls J T, Martín-Moreno L, Pepper M, Frost J E F, Ritchie D A and Jones G A C 1991 *Phys. Rev.* B **44** 10973

[9] Kristensen A, Jensen J B, Zaffalon M, Sørensen C B, Reimann S M, Lindelof P E, Michel M and Forchel A 1998 *J. Appl. Phys.* **83** 607

[10] Graham A C, Pepper M, Simmons M Y and Ritchie D A 2005 *Phys. Rev.* B **72** 193305
[11] Molenkamp L W, Gravier T, van Houten H, Buijk O J A, Mabesoone M A A and Foxon C T 1992 *Phys. Rev. Lett.* **68** 3765–8
[12] van Houten H, Molenkamp L W, Beenakker C W J and Foxon C T 1992 *Semicond. Sci. Technol.* **7** B215–21
[13] Mott N F and Jones H 1936 *The Theory of the Properties of Metals and Alloys* 1st edn (Oxford: Clarendon)
[14] Appleyard N J, Nicholls J T, Pepper M, Tribe W R, Simmons M Y and Ritchie D A 2000 *Phys. Rev.* B **62** R16275–8
[15] Sivan U and Imry Y 1986 *Phys. Rev.* B **33** 551–8
[16] Butcher P N 1990 *J. Phys.: Condens. Matter* **2** 4869
[17] Proetto C R 1991 *Phys. Rev.* B **44** 9096–9
[18] Lunde A M and Flensberg K 2005 *J. Phys.: Condens. Matter* **17** 3879–84
[19] Appleyard N J, Nicholls J T, Tribe W R, Simmons M Y and Pepper M 2000 *Physica* E **6** 534–7
[20] Appleyard N J, Nicholls J T, Simmons M Y, Tribe W R and Pepper M 1998 *Phys. Rev. Lett.* **81** 3491–4
[21] Chiatti O, Nicholls J T, Proskuryakov Y Y, Lumpkin N, Farrer I and Ritchie D A 2006 *Phys. Rev. Lett.* **97** 056601–4
[22] Çipiloğlu M A and Turgut S 2004 *J. Phys.: Condens. Matter* **16** 3671
[23] Pendry J 1983 *J. Phys. A: Math. Gen.* **16** 2161
[24] Rego L G C and Kirczenow G 1998 *Phys. Rev. Lett.* **81** 232–5
[25] Schwab K, Henriksen E A, Worlock J M and Roukes M L 2000 *Nature* **404** 974–7
[26] Meschke1 M, Guichard W and Pekola J P 2006 *Nature* **444** 187–90
[27] Fazio R, Hekking F W J and Khmelnitskii D E 1998 *Phys. Rev. Lett.* **80** 5611
[28] Rejec T, Ramšak A and Jefferson J H 2002 *Phys. Rev.* B **65** 235301
[29] Thomas K J, Nicholls J T, Pepper M, Tribe W R, Simmons M Y and Ritchie D A 2000 *Phys. Rev.* B **61** R13365
[30] Crook R, Prance J, Thomas K J, Chorley S J, Farrer I, Ritchie D A, Pepper M and Smith C G 2006 *Science* **312** 1359–62
[31] Matveev K A 2004 *Phys. Rev. Lett.* **92** 106801
[32] Matveev K A 2004 *Phys. Rev.* B **70** 245319